Effects of Annealing and Doping on Nanostructured Bismuth Telluride Thick Films

Shanghua Li,[†] Hesham M. A. Soliman,[†,§] Jian Zhou,[†] Muhammet S. Toprak,*[,†] Mamoun Muhammed,[†] Dieter Platzek,[‡] Pawel Ziolkowski,[‡] and Eckhard Müller[‡]

Department of Microelectronics and Applied Physics, Royal Institute of Technology (KTH), Department of Microelectronics and Applied Physics, SE-16440 Stockholm, Sweden and German Aerospace Center (DLR), Institute of Materials Research, D-51170 Cologne, Germany

Received March 10, 2008. Revised Manuscript Received April 30, 2008

Bismuth telluride is the state-of-the-art thermoelectric (TE) material for cooling applications with a figure of merit of ~1 at 300 K. There is a need for the development of TE materials based on the concept of thick films for miniaturized devices due to mechanical and manufacturing constraints for the thermoelement dimensions. We reported earlier a method for the fabrication of high-quality nanostructured bismuth telluride thick films with thickness from 100 to 350 μm based on electrochemical deposition techniques. In this paper, annealing is performed to further improve the TE performance of the nanostructured bismuth telluride thick films and n/p-type solid solutions are successfully fabricated by doping Se and Sb, respectively. The conditions for both annealing and doping for the thick films are investigated, and the effects of annealing and doping on morphology, crystalline phase, grain size, Seebeck coefficient, homogeneity, electrical conductivity, and power factor of the bismuth telluride thick films have been studied.

1. Introduction

Group 15 chalcogenide compounds have received considerable attention for more than three decades due to their potential application in the area of thermoelectric (TE) cooling. Thermoelectric materials can be utilized as electric generators or coolers in several applications, such as power generation systems and microcoolers,[1] CCD technologies,[2] and infrared detectors.[3] The thermoelectric figure of merit, ZT, can be expressed as $S^2T\sigma/\lambda$, where S is the Seebeck coefficient, σ is the electrical conductivity, T is the temperature, and λ is the thermal conductivity. Among the various thermoelectric materials, bismuth telluride (Bi_2Te_3), a group 15 chalcogenide compound, has been a main focus of research because of its superior ZT near room temperature in bulk form.

In our previous work[4] we introduced the advantages of the bismuth telluride thick film concept over conventional bulk materials. Use of a thick film is more suitable for application in devices covering large areas and operating at small to moderate temperature differences (20−200 K).[5,6] Thick film based devices have technological advantages over conventional TE module technology, where there are practical problems in fabricating pellets with lengths of few hundreds of micrometers. On the other hand, there are serious limitations on the use of thin films if applied to larger areas due to the need of draining of the released heat. This problem can be avoided by use of the thick film concept, where the influence of electrical and, in particular, thermal contact and spreading resistance is kept low. Thus, high efficiency and a high coefficient of performance (COP) can be achieved by using thick films with flux quantities being about 1 order of magnitude larger than that of conventional devices. By control of the film thickness, ideal tuning of the flux quantities to the specific application is feasible, ensuring efficient operation. We reported the fabrication of thick stoichiometric Bi_2Te_3 films comprised of nanostructured building blocks by the electrodeposition method. The thick films are very homogeneous n-type TE materials with a Seebeck coefficient around -70 μV K^{-1} as measured by Seebeck microscopy (SMP).

It has been reported that annealing can have an effect on the thermoelectric performance.[7–9] Annealing can be used to alter the defect concentration of the materials, thereby

* To whom correspondence should be addressed. Phone: +46-8-7908158. Fax: +46-8-7909072. E-mail: toprak@kth.se.
[†] Royal Institute of Technology (KTH).
[‡] Institute of Materials Research.
[§] Present address: Institute of Advanced Technology and New Materials, Mubarak City for Scientific Research and Technology Applications, P.O. Box 21934, New Borg El-Arab City, Alexandria, Egypt.

(1) Rowe, D. M.; Bhandari, C. M. *Modern Thermoelectrics*; Reston: Reston, VA, 1983.
(2) Shafai, C.; Brett, J. *Vac. Sci. Technol. A* **1997**, *15*, 2798.
(3) Min, G.; Rowe, D. M. *Solid-State Electron.* **1999**, *43*, 923.
(4) Li, S.; Toprak, M. S.; Soliman, H. M. A.; Zhou, J.; Muhammed, M.; Platzek, D.; Müller, E. *Chem. Mater.* **2006**, *18*, 3627.
(5) Fleurial, J. P.; Snyder, G. J.; Patel, J.; Herman, J. A.; Giauque, P. H.; Phillips, W. M.; Ryan, M. A.; Shakkottai, P.; Kolawa, E. A.; Nicolet, M. A. *Proceedings of the 18th International Conference on Thermoelectrics*, Baltimore, MD, Aug 29–Sept 2, 1999; IEEE Cat. No. 99TH8407: Piscataway, NJ, 1999, p 294.
(6) Fleurial, J. P.; Snyder, G. J.; Patel, J.; Herman, J. A.; Caillat, T.; Nesmith, B.; Kolawa, E. A. *AIP Conf. Proc.* **2000**, *504* (Space Technology and Applications International Forum Proceedings), 1500.
(7) Schultz, J. M.; McHugh, J. P.; Tiller, W. A. *J. Appl. Phys.* **1962**, *33*, 2443.
(8) Yamashita, O.; Sugihara, S. *J. Mater. Sci.* **2005**, *40*, 6439.
(9) Lee, D. M.; Lim, C. H.; Cho, D. C.; Lee, Y. S.; Lee, C. H. *J. Electron. Mater.* **2006**, *35*, 360.

10.1021/cm800696h CCC: $40.75
Published on Web 06/11/2008

altering the carrier concentration.[10] However, the TE properties of bismuth telluride-based compounds are not changed by only the carrier concentration but also by grain size and grain orientation, which will also be altered during the annealing process. Therefore, in order to optimize the TE figure of merit, *ZT*, of the bismuth telluride thick films the effects of annealing should be studied.

By varying the composition with slight deviations from its stoichiometric composition (Bi_2Te_3), bismuth telluride can be tailored as n-type ($Bi_{2-x}Te_3$) or p-type ($Bi_{2+x}Te_3$). However, the *ZT* of stoichiometric Bi_2Te_3 is not comparable with that of the state-of-the-art bismuth telluride-based systems made by doping other elements in various fabricating processes. It was suggested that structural doping introduces lattice short-range distortions, leading to a significant decrease in the lattice thermal conductivity, without affecting the power factor P ($P = S^2\sigma$).[11] As a result, solid solutions as $(Bi_{1-x}Sb_x)_2Te_3$ and $Bi_2(Te_{1-x}Se_x)_3$ are widely used in various compositions to shift the properties to certain temperature ranges.[12,13] Another way to improve the *ZT* of bismuth telluride compounds is doping a solid solution system with additional elements, forming secondary phase precipitated in the matrix, so that the carrier concentration can be adjusted and utilized to increase the band gap of the systems to avoid the ambipolar contribution to the thermal conductivity.[12–15] To date, the highest *ZT* at room temperature was 1.06 in the p-type $(Bi_{0.25}Sb_{0.75})_2Te_3$ doped with 4 wt % excess Te and 0.05 wt % Ge[12] and 1.75 wt % excess Se alone[13] and 0.96 in the n-type $(Bi_{0.25}Sb_{0.75})_2(Te_{0.95}Se_{0.05})_3$ solid solution doped with 0.16 wt % SbI_3.[14] Recently, the highest *ZT* of 1.14 at 300 K for the p-type $(Bi_{0.25}Sb_{0.75})_2(Te_{0.97}Se_{0.03})_3$ has been reported by Ettenberg et al.,[16] and a significantly high *ZT* of 1.19 at 298 K for the n-type $Bi_2(Te_{0.94}Se_{0.06})_3$ doped with 0.068 wt % I and 0.017 wt % Te has been reported by Yamashita et al.[8,15]

In this study, annealing was performed by heating the as-deposited bismuth telluride thick films at elevated temperature under a reductive atmosphere. Doping of bismuth telluride with additional elements was realized by electrodeposition with addition of respective element compounds into the electrolyte. The conditions for both annealing and doping for the thick films are investigated, and the effects of annealing and doping on morphology, crystalline phase, grain size, Seebeck coefficient, homogeneity, electrical conductivity, and power factor of the bismuth telluride thick films have been studied.

2. Experimental Section

Thick Film Fabrication. Thick films of bismuth telluride were either potentiostatically or galvanostatically electrodeposited onto gold sputtered-aluminum substrates as proposed in our previous work.[4] A gold layer (~100 nm thick) was sputtered onto one side of a piece of aluminum foil (0.1 mm thick, $1.5 \times 1.5 = 2.25$ cm^2, Riedel-de Haën) to serve as the working electrode (cathode) for electrodeposition. A three-electrode conventional electrochemical cell was used for the deposition of bismuth telluride with Pt foil (~8 cm^2) as the counter electrode (anode) and SCE as the reference electrode with a cathode−anode separation distance of 2 cm. Ar gas was bubbled into the electrolyte for 10 min to remove oxygen from the solution prior to electrodeposition and continued throughout the experiment at a low rate (~10 mL/min). Electrodeposition was carried out using an EG&G PAR model 263A potentiostat/galvanostat at room temperature (~298 K) either potentiostatically or galvanostatically with regular monitoring of the cathodic current and potential, respectively. Typical electrodeposition duration was around 24 h. Finally, the deposited films were removed from the electrolyte and rinsed in three steps: 0.1 M HNO_3 solution (pH ≈ 1), deionized water, and ethanol followed by drying in air.

For the deposition of stoichiometric Bi_2Te_3 thick films, the electrolyte contained 0.013 M BiO^+ and 0.01 M $HTeO_2^+$ in 1 M HNO_3. The potentiostatic electrodeposition was performed at −50, −75, −120, −150, and −200 mV, and for the galvanostatic electrodeposition, a current density of 3.3 mA/cm^2 was used while a high potential of around 1.9 V between the cathode and the anode was applied.

Annealing. To determine annealing conditions, thermal analysis including thermogravimetric analysis (TGA, TGA Q500, TA Instruments, Inc.) and differential scanning calorimetry (DSC, DSC 2920, TA Instruments, Inc.) are performed to understand the thermal behavior of the thick films during heating. Annealing was carried out by heating the thick films (~200 μm) at 300 °C for different durations under a reductive atmosphere (H_2) to avoid oxidation. After annealing, forced cooling was applied on the exterior of tube furnace to ensure the precise duration of the annealing process.

Doping. Thick films of bismuth telluride solid solutions as $Bi_2(Te_{1-x}Se_x)_3$ ($x \approx 0.05$) and $(Bi_{1-y}Sb_y)_2Te_3$ ($y \approx 0.75$) were prepared by varying the composition of the electrolytic solutions. For the deposition of $Bi_2(Te_{1-x}Se_x)_3$ ($x \approx 0.05$) thick films (~200 μm), galvanostatic deposition was applied with a current density of 3.3 mA/cm^2 and the electrolyte contained 0.013 M BiO^+, 0.009 M $HTeO_2^+$, and 0.001 M H_2SeO_3 in 1 M HNO_3. However, for $(Bi_{1-x}Sb_x)_2Te_3$ ($y \approx 0.75$), only thin films (less than 1 μm) could be obtained from the electrolyte containing 0.0019 M BiO^+, 0.01 M $HTeO_2^+$, 0.0056 M SbO^+, and 0.2 M tartaric acid (99%, Aldrich) in 1 M HNO_3 using potentiostatic electrodeposition at −75, −100, and −200 mV vs SCE. All other conditions were kept the same as that of stoichiometric bismuth telluride thick films. Annealing was not performed on the doped films.

Characterization. XRD patterns of the films were obtained using a Philips PW 1012/20 and 3020 diffractometer with Cu Kα radiation. The average crystallite size, D, could be calculated from the peak broadening of the diffraction pattern using Scherrer's equation,[17] $D = 0.9\lambda/(\beta \cos \theta)$, where β is the pure diffraction line width, full width at half-maximum, and λ is the X-ray wavelength (Cu Kα_1, $\lambda = 1.54056$ Å).

Electrodeposited bismuth telluride thick films were imaged with scanning electron microscopy (SEM, JEOL JSM-888) equipped with an energy-dispersive X-ray spectrometer (EDS), which was

(10) Gerovac, N.; Snyder, G. J.; Caillat, T. *Proceedings of the 21st International Conference on Thermoelectrics*, Long Beach, CA Aug 25–Aug 29, 2002, IEEE Cat. No. 02TH8657: Piscataway, NJ, 2002; p 31.
(11) Ioffe, A. F.; Airapetiants, S. V.; Kolomoets, N. V.; Stil'bans, L. S. *Dokl. Akad. Nauk. SSSR* **1956**, *106*, 981.
(12) Smirous, K.; Stourac, L. *Z. Naturforsch.* **1959**, *14a*, 848.
(13) Rosi, F. D.; Hockings, E. F.; Lindenblad, N. E. *RCA Rev.* **1961**, *22*, 82.
(14) Yim, W. M.; Rosi, F. D. *Solid-State Electron.* **1972**, *15*, 1121.
(15) Yamashita, O.; Tomiyoshi, S. *Jpn. J. Appl. Phys.* **2003**, *42*, 492.
(16) Ettenberg, M. H.; Jesser, W. A.; Rosi, E. D. *Proceedings of the 15th International Conference on Thermoelectrics*, Pasadena, CA, Mar 26–29, 1996, IEEE: Piscataway, NJ, 1996; p 52.
(17) Klug, H. P.; Alexander, L. E. *X-ray diffraction procedures*; John Wiley & Sons Inc.: New York, 1954.

used for composition analysis. The thickness of the films was determined by measuring the cross-section of the films.

TE Evaluation. The Seebeck coefficient of different thick film samples prepared by electrodeposition and annealing process has been measured. The Seebeck microprobe (SMP) is a device for measuring the Seebeck coefficient on the sample surface with a spatial resolution down to 10−50 μm (depending on the thermal conductivity of the material). A heated probe tip is positioned onto the sample surface. The sample is fixed in good electrical and thermal contact to a heat sink and connected to another thermocouple measuring the sink temperature. The heat flow from the probe tip to the sample causes a local temperature gradient in the vicinity of the tip. Mounting the probe to a three-dimensional micropositioning system allows for determination of the thermopower at each microposition of the sample surface. The result is a two-dimensional image of the Seebeck coefficient.[18,19] Special sample holders have been developed to mechanically fix thick films as well as ensure simultaneously good electrical and thermal contact as a precondition for a high-quality measurement. The SMP apparatus has been improved by adding an electronic contact detection system so that the probe tip will stop its movement immediately after touching the sample to avoid destruction of the films.

Seebeck coefficient measurement is a tool to detect the distribution of different electrically active components in the materials. It is capable of detecting functional inhomogeneities, different phases, even small differences in doping concentration, which cannot be detected by other surface analysis methods such as SEM, EDS, etc. Measuring the Seebeck coefficient of films can be difficult because the local temperature gradient caused by the probe tip can also heat the materials of the supporting substrate, yielding an integration of the Seebeck coefficient of the sample and the substrate. If the substrate has a very low thermal coupling, this effect will be negligible. The TE thick films were deposited on a Au-coated Al substrate with a very good thermal coupling, which could lead to erroneous measurements. Taking into account the thickness of the samples of more than 100 μm, this effect will disappear or at least attenuate because the local temperature gradient will not exceed a certain depth of an estimated 50 μm in bismuth telluride. Recent results show that indeed it is now possible to measure the influence of a substrate and estimate the depth of the temperature gradient.[20]

The electrical conductivity has been measured on the as-deposited stoichiometric Bi_2Te_3 thick films by means of in-line four-point probe rising from room temperature to 300 °C. Thus, the annealing effects on the electrical conductivity of the thick films can be studied. An ac current of several milliamps is applied to the outer contact probes, and the voltage is measured with the inner probes. The distance between all adjacent probes is equal. A numerical correction factor (Valdez factor) is applied to take into account the particular geometry of the sample. To eliminate the influence of the metallic substrate on the electrical conductivity measurement, only free-standing films were considered in this work. Because the toughness of the deposited free-standing films is not high enough, it is difficult to apply the four-point probe without destroying the film. Therefore, electrical conductivity measurement was limited to several free-standing films that occasionally possess better toughness, and during the measurements situations such as bad contact always happened. Unfortunately, electrical conductivity measurements have only been successful on stoichiometric Bi_2Te_3 thick films but not yet on doped bismuth telluride solid solutions. The method for measuring the electrical conductivity of thick films is still under development. Thermal conductivity, although very difficult to perform on films, is still under investigation and will be reported elsewhere upon successful completion of the measurements.

3. Results and Discussion

Annealing Effects. Before annealing, thermal analysis including TGA and DSC was conducted to understand the thermal behavior of the bismuth telluride thick films. TGA analysis (Figure S1A) shows a distinct weight increase peak after 400 °C which is attributed to partial oxidation of the film and confirmed with XRD measurements. DSC analysis (Figure S1B) exhibits an exothermic peak around 150 °C, indicating recrystallization of materials with nanosized grains. In order to verify that the samples were heated up to 200 °C, where no oxidation was detected by XRD; thereafter, after cooling to room temperature, the samples are reheated from room temperature to 550 °C, where no such peak is observed anymore. This irreversible recrystallization process at relatively lower temperature is a typical behavior of materials with nanosized features. The broad weak exothermic peak between ∼200 and 400 °C indicates a microstructural change of the film, and the continuous exothermic line starting after around 450 °C is attributed to be the partial oxidation of the film which is consistent with the result of TGA (Figure S1A). Yamashita et al.[15] performed a series of annealing tests under different temperatures and suggested an optimum annealing temperature of 400 °C. Considering that the high-temperature annealing process causes growth of grain size and the smaller size proved to be favored for TE materials since nanostructuring greatly reduces the thermal conductivity resulting in higher ZT,[21,22] a lower temperature is preferred for the annealing of thick films. Therefore, the annealing temperature chosen for the as-deposited bismuth telluride thick films was set to 300 °C. Since TGA suggested a potential problem of oxidation, a reductive atmosphere (H_2) is necessary during the annealing process.

Two samples of the as-deposited bismuth telluride thick films (∼200 μm) were annealed at 300 °C for 2 and 5 h under a hydrogen atmosphere. Figure 1 exhibits the effects of annealing on the surface morphology of the thick films. SEM images of as-deposited bismuth telluride thick films (Figure 1A) obtained by galvanostatic electrodeposition show that the films are comprised of needle-like structures with features in the nanorange (∼20−30 nm in width). After

(18) Reinshaus, P.; Süβmann, H.; Bohm, M.; Schuck, A.; Dietrich, T. *Proceedings of the 2nd European Symposium on Thermoelectrics: Materials, Processing Techniques, and Applications*, Sept 15−17, http://home.agh.edu.pl/∼ets2004/proceedings/Stiewe.PDF. 2004, Krakow, Poland; European Thermoelectric Society: 2004; p 90.

(19) Platzek, D.; Zuber, A.; Stiewe, C.; Bähr, G.; Reinshaus, P.; Müller. E. *Proceedings of the 22nd International Conference on Thermoelectrics*, LaGrande-Motte, France, Aug 17−21, 2003; IEEE: New York, 2004; p 528.

(20) Platzek, D.; Karpinski, G.; Stiewe, C.; Ziolkowski, P.; Stordeur, M.; Engers, B.; Müller, E. *3rd European Conference on Thermoelectrics*, Nancy, France, Sept 1−2, 2005; European Thermoelectric Society: 2005, http://www.lpm.u-nancy.fr/ECT2005/proceedings.htm.

(21) Toprak, M. S.; Stiewe, C.; Platzek, D.; Williams, S.; Bertini, L.; Müller, E.; Gatti, C.; Zhang, Y.; Rowe, M.; Muhammed, M. *Adv. Funct. Mater.* **2004**, *14*, 1189.

(22) Stiewe, C.; Bertini, L.; Toprak, M. S.; Christensen, M.; Platzek, D.; Williams, S.; Gatti, C.; Müller, E.; Iversen, B. B.; Muhammed, M.; Rowe, D. M. *J. Appl. Phys.* **2005**, *97*, 044317.

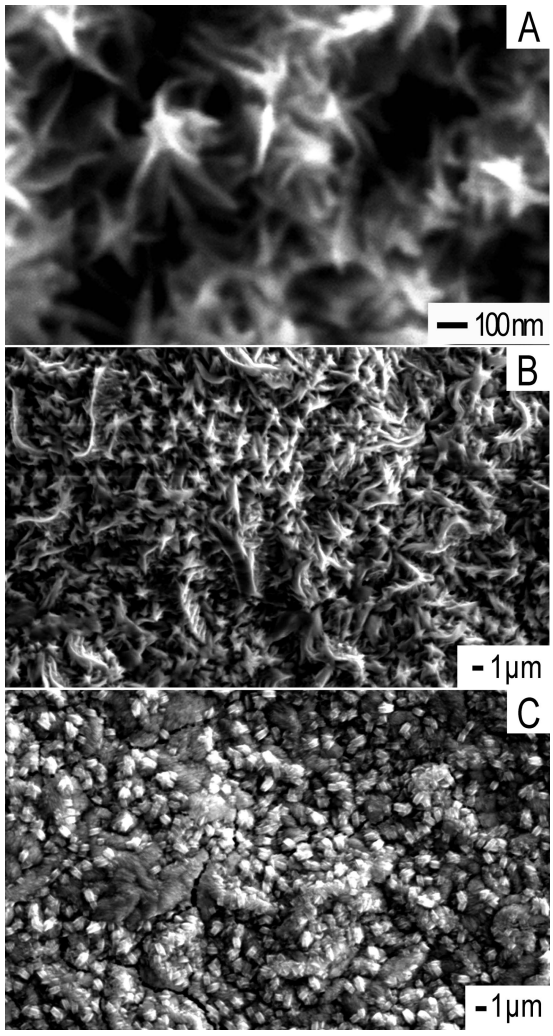

Figure 1. SEM images of (A) galvanostatically deposited stoichiometric Bi_2Te_3 thick film from 0.013 M BiO^+, 0.01 M $HTeO_2^+$, and 1 M HNO_3 in the electrolyte with a current density of 3.3 mA/cm^2 (ref 4, Figure 3A), (B) bismuth telluride thick film annealed at 300 °C for 2 h under H_2 atmosphere, and (C) bismuth telluride thick film annealed at 300 °C for 5 h under H_2 atmosphere.

annealing at 300 °C for 2 h, the needle-like structures were maintained while the grain size increased dramatically (∼40−100 nm in width, Figure 1B). However, after annealing at 300 °C for 5 h, all the needle-like structures turned into granular square structures (above 100 nm in diameter) since needle-like structures have a bigger surface area and therefore are less stable than granular square structures. The exact number of the grain size was difficult to estimate from SEM micrographs due to the irregular shapes of the grain and the poor resolution of SEM. EDS analysis confirmed that all the films are stoichiometric Bi_2Te_3, and no oxidation took place during the annealing process.

Figure 2 shows the XRD patterns of the as-deposited bismuth telluride thick film and annealed films at 300 °C for different durations. The XRD patterns exhibit polycrystalline bismuth telluride with (110) as a prominent plane parallel to the substrate. According to the standard ICDD PDF card (No. 00-008-0021), all of the detected peaks are indexed as those from the rhombohedral Bi_2Te_3 crystal [space group ($R\bar{3}$ m) (166)]. However, the intensity ratios of the peaks are not in agreement with those obtained by XRD on a ground sample, indicating an orientational effect in the film growth.[23] For annealed films, the peak becomes much narrower than the as-deposited film, which indicates a substantial increase of the grain size. The average crystallite size of as-deposited bismuth telluride thick film calculated by Scherrer's equation is ∼15 nm, while for a 2 h annealed film it is ∼45 nm and increases to ∼77 nm for a 5 h annealed film.

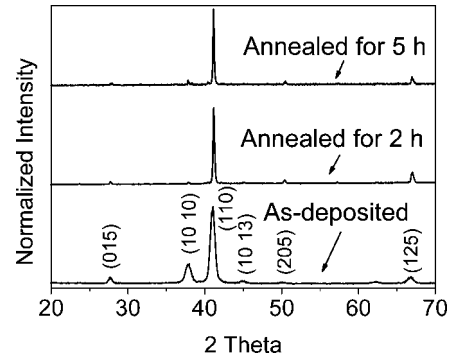

Figure 2. XRD patterns of as-deposited film and annealed films at 300 °C for 2 and 5 h.

The Seebeck coefficient of different Bi_2Te_3 thick films (as deposited and annealed) was measured by SMP, and results are shown in Figure 3. All films are n-type, and annealed films at 300 °C show a higher average Seebeck coefficient (ca. -130 μV K^{-1} for 2 h and ca. -120 μV K^{-1} for 5 h) than as-deposited film (ca. -70 μV K^{-1}), which is in agreement with Lee et al.[9] The influence of the Seebeck coefficient by annealing is attributed to the combination of improved crystallinity and changes in defect concentration. It is reported that annealing increases thermopower and resistivity consistent with a decrease in carrier concentration.[24] Yamashita et al.[8] summarized that annealing has had a favorable effect on the improvement in *ZT* of n-type bismuth telluride bulk compounds but an adverse effect on p-type. From the spatial distribution (Figure 3A, 3C, and 3E) and abundance distribution (Figure 3B, 3D, and 3F) of the Seebeck coefficient measured on the films, it is evident that the as-deposited thick film has a very high homogeneity in the Seebeck coefficient with the abundance distribution showing a half width of below 1 μV K^{-1}, while film annealed for 2 h is less homogeneous with the abundance distribution showing a half width of around 3 μV K^{-1}, and film annealed for 5 h is even less homogeneous with the abundance distribution showing a half width of around 10 μV K^{-1}. In Figure 3C and 3E there is a diagonal line with a low Seebeck coefficient compared to the rest of the film. This is not due to the annealing process and not representative of the film but associated to the SMP measurement flaw. It can be concluded that annealing enhances the Seebeck coefficient but reduces the homogeneity, and annealing for longer duration could not enhance the Seebeck coefficient further but decreases the homogeneity.

(23) Chaouni, H.; Magri, P.; Bessieres, J.; Boulanger, C.; Heizmann, J. *J. Proc. Icotom* **1994**, *10*, 1371.
(24) Stoltz, N. G.; Snyder, G. J. *Proceedings of the 21nd International Conference on Thermoelectrics*, Long Beach, CA, Aug 25–29, 2002, IEEE Cat. No. 02TH8657: Piscataway, NJ, 2002; 28.

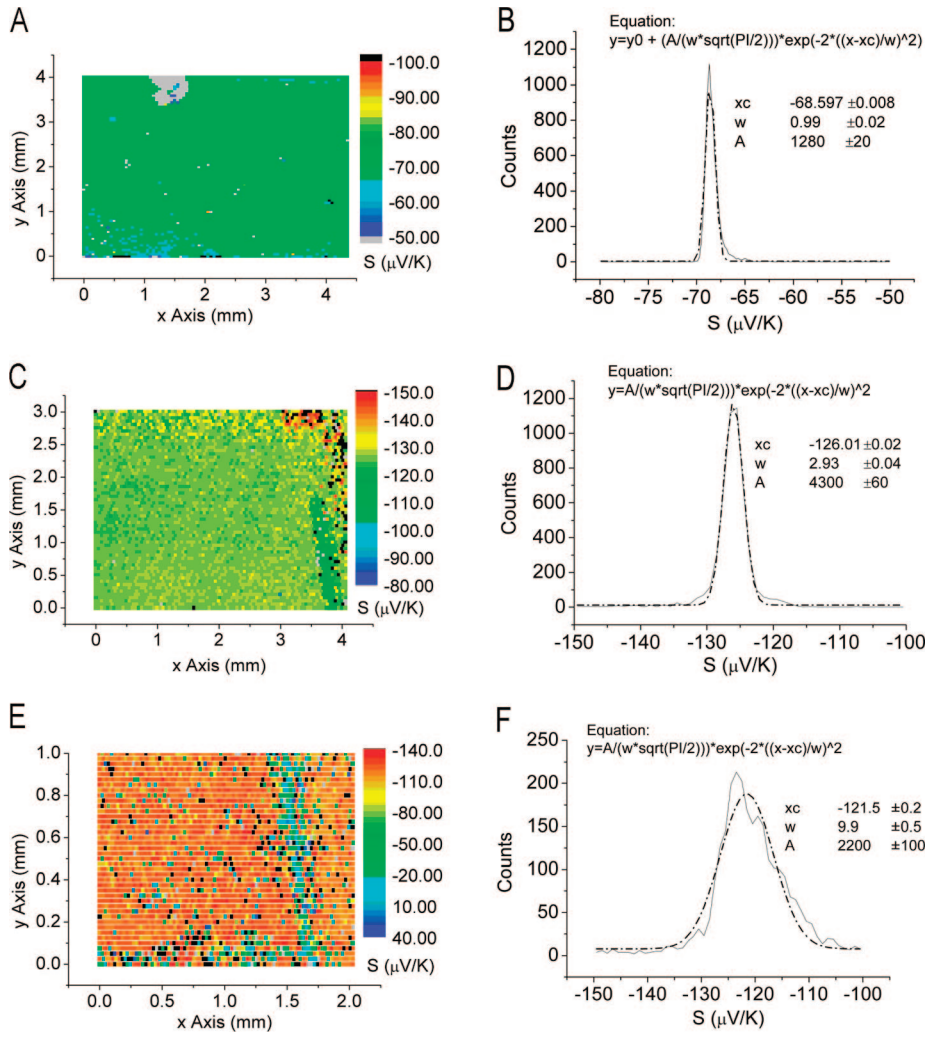

Figure 3. Spatial distribution and abundance distribution of the Seebeck coefficient measured on (A, B) as-deposited bismuth telluride thick film (ref 4, Figure 7), (C, D) as-deposited film annealed for 2 h, and (E, F) as-deposited film annealed for 5 h.

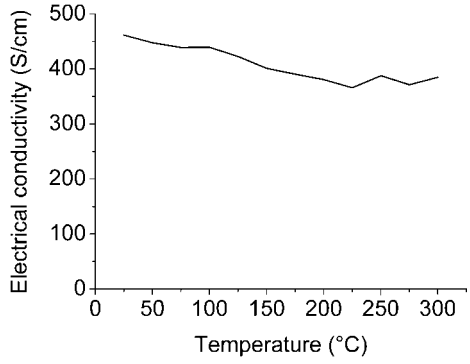

Figure 4. Electrical conductivity of free-standing stoichiometric Bi_2Te_3 thick films from room temperature to 300 °C.

The electrical conductivity of free-standing stoichiometric Bi_2Te_3 thick films is ~450 S cm^{-1} at room temperature, as shown in Figure 4, and slightly decreases to 400 S cm^{-1} when heated to higher temperatures up to 300 °C. The same behavior has been reported by others and is attributed to the reduction in carrier concentration due to annealing.[8–10,15,24] Since the Seebeck coefficient of the as-deposited thick films is enhanced from around -70 μV K^{-1} at room temperature to around -130 μV K^{-1} after annealing at 300 °C, the power factor ($S^2\sigma$) of the as-deposited thick films can be calculated to be around 220 μW m^{-1} K^{-2} at room temperature and will increase to around 680 μW m^{-1} K^{-2} after annealing at 300 °C.

Thermal conductivity can be divided into two parts: electronic thermal conductivity and lattice thermal conductivity, $\lambda = \lambda_e + \lambda_l$. Electrical thermal conductivity, λ_e, can be calculated according to the Wiedemann−Franz law, $\lambda_e = L\sigma T$, where σ is the electrical conductivity, T is the temperature, and L is the Lorenz number. Since the electrical conductivity of the as-deposited bismuth telluride thick films does not change much during annealing, the electrical component of the thermal conductivity should also not be altered much by annealing. The lattice thermal conductivity depends on the grain size and concentration of phonon scattering defects.[25] During annealing the nanosized grains of as-deposited bismuth telluride thick films grow; thus, there is less phonon scattering by grain boundaries, resulting in higher lattice thermal conductivity. However, the actual effect of annealing on thermal conductivity is unknown since measurements of the thermal conductivity on thick films are unavailable yet.

(25) Volckmann, E. H.; Goldsmid, H. J.; Sharp, J. *Proceedings of the 15th International Conference on Thermoelectrics*, Pasadena, CA, Mar 26–29, 1996, IEEE: Piscataway, NJ, 1996; p 22.

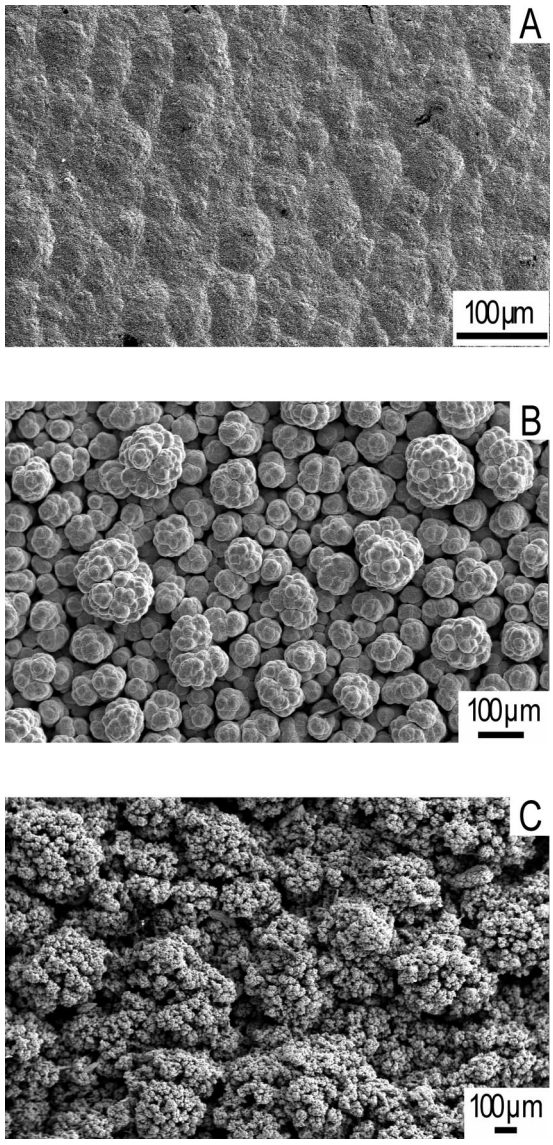

Figure 5. SEM images of (A) galvanostatically electrodeposited stoichiometric Bi_2Te_3 thick film from 0.013 M BiO^+, 0.01 M $HTeO_2^+$, and 1 M HNO_3 in the electrolyte with a current density of 3.3 mA/cm^2, (B) galvanostatically electrodeposited Se-doped bismuth telluride thick film from 0.013 M BiO^+, 0.009 M $HTeO_2^+$, 0.001 M H_2SeO_3, and 1 M HNO_3 in the electrolyte with a current density of 3.3 mA/cm^2, (C) potentiostatically electrodeposited Sb-doped bismuth telluride thin film from 0.0019 M BiO^+, 0.01 M $HTeO_2^+$, 0.0056 M SbO^+, 0.2 M tartaric acid, and 1 M HNO_3 in the electrolyte with a potential of −100 mV.

Doping Effects. Thick films of n-type Se-doped bismuth telluride solid solutions could be galvanostatically electrodeposited by slightly varying the composition of the electrolyte used for deposition of stoichiometric Bi_2Te_3. This is possible due to the following reasons. (1) The reduction process for electrolytes containing H_2SeO_3 is comparable to that without H_2SeO_3; $Te_{1-x}Se_x$ solid solutions are formed instead of elemental Te.[26] (2) The amount of Se required for the state-of-the-art n-type $Bi_2(Te_{1-x}Se_x)_3$ ($x \approx 0.05$)[15] at room temperature is too little. However, p-type Sb-doped bismuth telluride solid solutions could not be produced by galvanostatic electrodeposition. This is also attributed to two reasons. (1) Sb(III) can hardly be dissolved together with Te(IV) and Bi(III) in HNO_3. Therefore, chelating agent such as tartaric acid is required to ensure the stability and solubility of Sb(III) with Bi(III) and Te(IV).[27] As a result, the reduction conditions for Sb(III) are very different from that for Bi(III) and Te(IV). (2) The amount of Sb required for the state-of-the-art p-type $(Bi_{1-y}Sb_y)_2Te_3$ ($y \approx 0.75$)[12] at room temperature is comparably large, 3 times of that for Bi. In fact, no Sb was found on the films after electrodeposition from the electrolyte containing a considerable amount of Sb(III) using typical galvanostatic conditions in this work. Therefore, potentiostatic electrodeposition had to be carried out for deposition of p-type Sb-doped bismuth telluride solid solutions, and cyclic voltammetry was used to find the appropriate potential range for deposition. As shown in Figure S2, two reduction waves were observed in the cathodic scan. The first level ranges between 50 and −10 mV, which would be representative of reduction of Te(IV) to Te as well as deposition of Bi_2Te_3.[27] The second level, ranging between −10 and −300 mV, is due to the further reduction of $HTeO_2^+$ to H_2Te, which would instantaneously react with both Bi^{3+} and SbO^+ to form the ternary deposition of $(Bi_{1-y}Sb_y)_2Te_3$.[28] The reduction potential of Sb(III) to Sb is usually more negative than bismuth and tellurium,[27] which explains why the deposited $(Bi_{1-y}Sb_y)_2Te_3$ is always powdery, since the nucleation reaction is constantly accompanied by hydrogen evolution from the reduction of both bismuth and tellurium. The overall cathodic reaction can be expressed as follows

$$3HTeO_2 + +(2-y)Bi^{3+} + ySbO^+ + (9+2y)H^+ + 18e^- \rightarrow Bi_{2-y}Sb_yTe_3 + (6+y)H_2O \quad (1)$$

As for the anodic scan, generally, multiple anodic peaks could be due to the stripping charge of the bulk deposit and the charge for a monolayer of bismuth telluride on the basal plane.[29] In addition, there are other possible explanations for this type of phenomenon, such as underpotential deposition, alloy formation with the substrate, diffusion of cations into the substrate, and the presence of more than one type of deposited bismuth telluride (such as epitaxial growth on different faces or nonepitaxial growth). In our case, two oxidation peaks observed at ∼210 and 560 mV were associated with oxidation of Bi to Bi(III) and Bi_2Te_3 to $HTeO_2^+$, respectively.[30] As a result, the potential range from −10 to −300 mV vs SCE was chosen for the potentiostatic electrodeposition of p-type Sb-doped bismuth telluride solid solutions. In this work, thin films (less than 1 μm) of p-type $(Bi_{1-y}Sb_y)_2Te_3$ ($y \approx 0.75$) have been successfully obtained by potentiostatic electrodeposition at −75, −100, and −200 mV, whereas thick film (above 100 μm) of p-type Sb-doped bismuth telluride solid solutions remained problematic, since the film became powdery when the thickness was increased.

(26) Martin-Gonzalez, M.; Snyder, G. J.; Prieto, A. L.; Gronsky, R.; Sands, T.; Stacy, A. M. *Nano Lett.* **2003**, *3*, 973.
(27) Frari, D. D.; Diliberto, S.; Stein, N.; Boulanger, C.; Lecuire, J. M. *Thin Solid Films* **2005**, *483*, 44.
(28) Huang, Q.; Wang, W.; Jia, F.; Zhang, Z. *J. Univ. Sci. Technol. Beijing (Materials)* **2006**, *13*, 3–277.
(29) Gu, P.; Pascual, R.; Shirkhanzadeh, M.; Saimoto, S.; Scott, J. D. *Hydrometallurgy* **1995**, *37*, 267.
(30) Martin-Gonzalez, M. S.; Prieto, A. L.; Gronsky, R.; Sands, T.; Stacy, A. M. *J. Electrochem. Soc.* **2002**, *149*, C546.

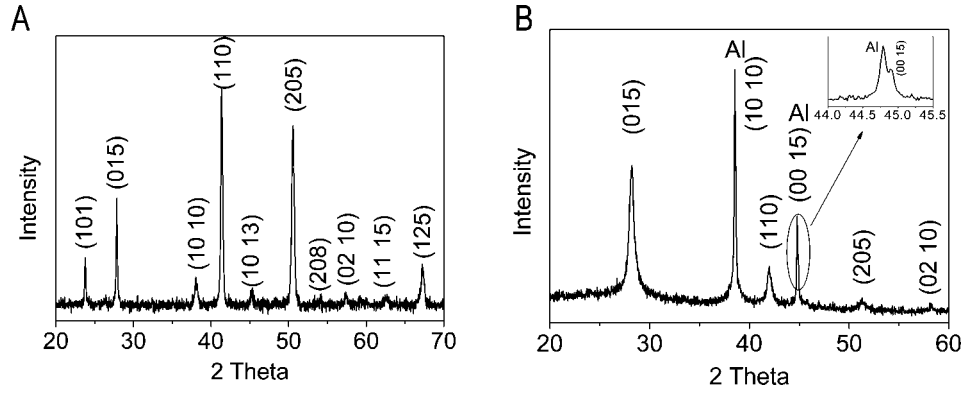

Figure 6. XRD patterns of (A) Se-doped bismuth telluride thick film and (B) Sb-doped bismuth telluride thin film. (Inset) Scale-up double peak at around 45, 2 theta values.

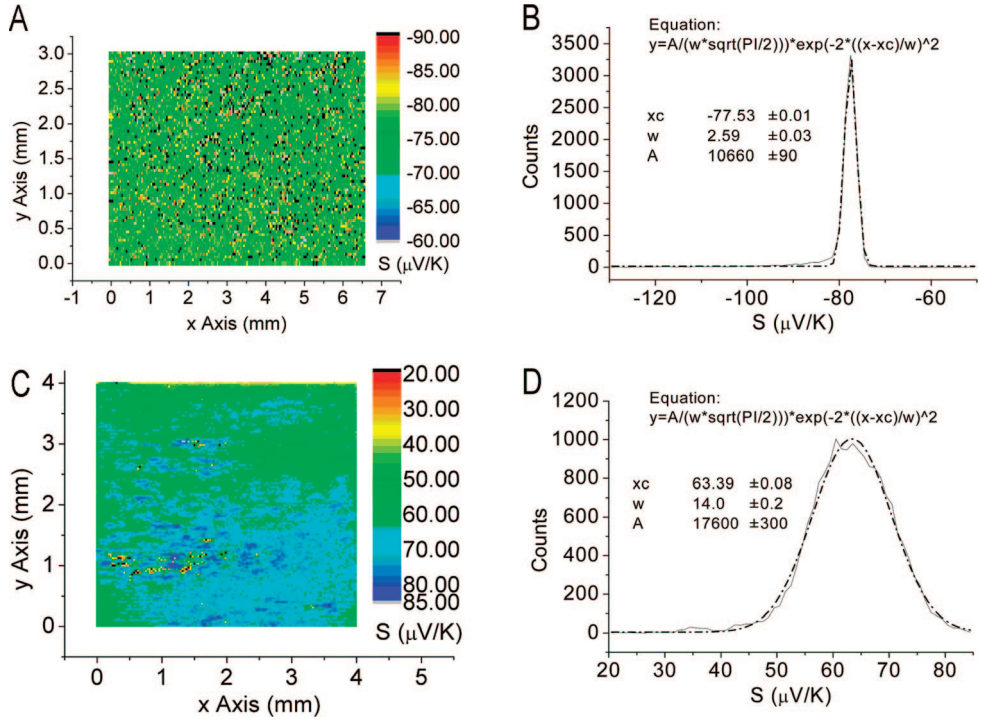

Figure 7. Spatial distribution and abundance distribution of the Seebeck coefficient measured on (A, B) Se-doped bismuth telluride thick films and (C, D) Sb-doped bismuth telluride thin films.

This problem could not be solved by introducing additives such as ethylene glycol, sodium dodecyl sulfate, DK-400, etc.

The as-deposited stoichiometric Bi_2Te_3 thick film exhibits metallic luster from the surface, while Se-doped bismuth telluride thick film and Sb-doped bismuth telluride thin film are gray and black, respectively. All samples exhibit similar microstructure; therefore, SEM images showing only the macroscopic morphology of stoichiometric Bi_2Te_3 thick film (~200 μm), Se-doped bismuth telluride thick film (~200 μm), and Sb-doped bismuth telluride thin film (less than 1 μm) are presented in Figure 5. Stoichiometric Bi_2Te_3 thick film (Figure 5A) has the most compact structure, while Se-doped bismuth telluride thick film (Figure 5B) is less compact, and Sb-doped bismuth telluride thin film (Figure 5C) is loose. EDS analysis showed the ratio between Bi, Te, and Se of Se-doped bismuth telluride thick films to be 41:53:6, which is close to the state-of-the-art n-type composition, $Bi_2(Te_{1-x}Se_x)_3$ ($x \approx 0.05$), at room temperature.[15] The ratio between Bi, Sb, and Te of Sb-doped bismuth telluride thin films is measured to be 10:29:61, which is close to the state-of-the-art n-type composition, $(Bi_{1-y}Sb_y)_2Te_3$ ($y \approx 0.75$), at room temperature.[12]

XRD analysis, shown in Figure 6, confirms that Se and Sb elements are doped into bismuth telluride solid solution system and not present as secondary phase. For Se-doped bismuth telluride thick films the crystal structure is very close to the undoped rhombohedral ($R\bar{3}m$) Bi_2Te_3 in accordance with the EDS data. All the peaks in the XRD pattern can be indexed as shown in Figure 6A. Compared to undoped rhombohedral Bi_2Te_3, a general shift of peaks to higher 2 theta values was observed since there is a contraction of the crystal structure as Te is replaced by the smaller Se atoms.[31] The average crystallite size of Se-doped bismuth telluride thick films calculated by Scherrer's equation is close to that of stoichiometric Bi_2Te_3 thick films. In addition, there is

(31) Shannon, R. D. *Acta Crystallogr.* **1976**, *A32*, 751.

texture in this nicely crystalline film leading to the altered intensities. For Sb-doped bismuth telluride thin films, two strong peaks at around 38.5 and 44.8 (2 theta value, Figure 6B) are detected due to the Al substrate. In fact, each of these peaks includes one overlapped peak (38.65 and 44.91, 2 theta value) from deposited Sb-doped bismuth telluride films (Figure 6B, inset). All the peaks that belong to Sb-doped bismuth telluride can be indexed to a rhombohedral $Bi_{0.4}Sb_{1.6}Te_3$ (ICDD No. 01-072-1836), in good agreement with the EDS data ($\sim Bi_{0.5}Sb_{1.5}Te_3$).

The Seebeck coefficient of bismuth telluride solid solutions (Se-doped thick films and Sb-doped thin films) was measured by SMP (Figure 7). Figure 7A shows that an average Seebeck coefficient of around $-80\ \mu V\ K^{-1}$ was obtained on Se-doped bismuth telluride thick films, which confirms that the Se-doped bismuth telluride thick films are n-type and the Seebeck coefficient is slightly higher in absolute value than stoichiometric Bi_2Te_3 thick films (ca. $-70\ \mu V\ K^{-1}$). However, the abundance distribution (Figure 7B) of the Seebeck coefficient on Se-doped bismuth telluride thick films shows a half width of around $3\ \mu V\ K^{-1}$, which is higher than that of stoichiometric Bi_2Te_3 thick films ($\sim 1\ \mu V\ K^{-1}$), indicating the inhomogeneity of the Se-doped film compared with that of stoichiometric Bi_2Te_3 thick films. The spatial distribution of the Seebeck coefficient measured on Sb-doped bismuth telluride thin films (Figure 7C) shows an average Seebeck coefficient of $+65\ \mu V\ K^{-1}$. p-Type thin films of bismuth telluride solid solutions were obtained by doping Sb into bismuth telluride system. The abundance distribution of the Seebeck coefficient on Sb-doped bismuth telluride thin films (Figure 7D) shows a half width of around $14\ \mu V\ K^{-1}$, indicating poor homogeneity.

4. Conclusions

In summary, annealing has been performed by heating the electrodeposited nanostructured TE bismuth telluride thick films at 300 °C under a reductive atmosphere. In this work, we successfully demonstrated the fabrication of n- and p-type nanostructured bismuth telluride films by doping Se and Sb, respectively. n-Type Se-doped bismuth telluride thick films and p-type Sb-doped bismuth telluride thin films have been obtained. The conditions for both annealing and doping for the thick films are investigated, and the effects of annealing and doping on morphology, crystalline phase, grain size, Seebeck coefficient, homogeneity, electrical conductivity, and power factor of the bismuth telluride thick films have been studied. These results are promising as the investigated conditions alter/improve some of the TE properties such as Seebeck coefficient and power factor while negatively affecting some other properties such as electrical conductivity and film homogeneity. There is still a need for optimization of the conditions in order to be able to improve the TE performance of the thick films based on nanostructured bismuth telluride system.

Acknowledgment. This work was supported by the European Community under contract number FP6-512805, IMS project, and Swedish Research Council (Vetenskapsrådet). The authors acknowledge Wubeshet Sahle for helpful discussion with X-ray crystallography. Advanced DSC analysis by TA Instruments Inc. is acknowledged. The fellowship from Knut and Alice Wallenbergs Foundation is also thankfully acknowledged (No: UAW2004.0224) by Dr. M.S. Toprak.

Supporting Information Available: Thermal analysis, TGA and DSC, of the as-deposited films and CV of electrolyte. This material is available free of charge via the Internet at http://pubs.acs.org.

CM800696H